# Heralded gate search with genetic algorithms for quantum computation

A. Chernikov [1], S. S. Sysoev [2], E. A. Vashukevich [1], and T. Yu. Golubeva [1]
[1]*Saint Petersburg State University, St. Petersburg 199034, Russia*
[2]*Leonhard Euler International Mathematical Institute, St. Petersburg 197376, Russia*

(Received 13 March 2023; accepted 21 June 2023; published 7 July 2023)

In this paper we present a genetic-algorithm-based search technique for linear optics schemes, performing two-qubit quantum gates. We successfully apply this technique to find heralded two-qubit gates and obtain schemes with performance parameters equal to the best currently known. Simple metrics are introduced which enable a comparison of schemes with different heralding mechanisms. The scheme performance degradation is discussed for the cases when detectors in the heralding part of the scheme are not photon-number resolving. We propose a procedure for overcoming this drawback which allows us to restore the reliable heralding signal even with non-photon-number-resolving detectors.

DOI: 10.1103/PhysRevA.108.012609

## I. INTRODUCTION

For more than 20 years photonic quantum-computational network development has remained a challenging task for the scientific community [1]. Photons as a platform for quantum information attract attention for various reasons: They are inexpensive, easily manipulated, reliably detected, transmitted, and can even be stored in a quantum memory [2,3]. Photons are our best choice for the task of avoiding decoherence since they almost never interact with each other, which, however, appears to be the source of the main obstacle when it comes to computations, since this interaction is necessary for controlled quantum gates.

The use of linear optics schemes with heralding is currently believed to be the most beneficial approach for the development of photonic quantum gates [4–6]. Such schemes are based on the principle of probabilistic gate actuation with a probability much lower than 100%. Performing the transformation on quantum systems of a larger dimension, linear optical circuits involve the detection of a certain pattern at the output of the circuit (heralding signal), indicating that the required operation is performed on unmeasured outputs. All detection outcomes in which this pattern is not implemented are considered unsatisfactory, which leads to a significant decrease in the gate actuation probability. Low actuation probabilities prevent effective heralded scheme scaling. To improve this situation, it has been proposed to use several identical schemes in place of one with the selection of correct outputs for further computation [7]. However, this approach not only is resource intensive (it involves a significant increase in the number of optical elements), but also requires signal delaying and use of fast switches. All these elements become a source of channel losses and additional noise.

The first linear optics entangling two-qubit gate was introduced by Knill *et al.* [8], along with the Knill-Laflamme-Milburn (KLM) protocol. This controlled-$Z$ (CZ) gate has an actuation probability of $1/16$ and a heralding mechanism implemented with four ancillary spatial modes and two ancillary photons. This result inspired great optimism and interest in the linear optics gate implementations, which in less than a year resulted in better implementation [9] of the CZ gate with an actuation probability of $2/27$ and a much simpler scheme architecture. Later in [10], O'Brien *et al.* achieved an even better actuation probability of $1/9$, though with a less reliable heralding event, with a postselection procedure.

Later progress in the area produced more gate architectures [11–15]. It was also proposed to use entangled ancillary photons [16–19] and Bell state measurements [20,21] to achieve higher probabilities. Schemes using auxiliary entangled photon states provide extremely high probabilities (up to $1/4$ [18]). However, if we include the input state generation into the scheme analysis, the advantage of such schemes does not seem obvious due to the low number of operations per unit of time due to the necessity of generation of a multiphoton state.

In this paper we exclude from consideration schemes with preentangled photons and concentrate on two types of heralding event: detection pattern in ancillary modes (like in [8,9]) and postselection with photons detection in signal (nonancillary) modes (like in [10]). Finding an effective optical scheme for a conditional gate has proven to be a complicated task, and the modern approach for handling complicated tasks is feeding them into a computer. With several natural restrictions, the task can be formulated as a global optimization problem, for which plenty of heuristics are currently available. We choose genetic algorithms, introduced in [22,23] and fruitfully employed for a diverse set of tasks ever since (see, for example, [24–27]). Here we present the results of the genetic algorithm application to the problem of finding the conditional gate scheme with best fidelity and probability in the KLM protocol.

We consider two well-known schemes that implement entangling gates in order to identify their features and discuss the various probabilities that characterize the gates. This opens up two different search strategies that we are implementing in this paper. In addition, we analyze the stability of the scheme to detection errors. We limit the outcomes to the act of distinguishing just two events on the detectors in the heralding channels: The absence of a click corresponds to the vacuum state of the field in the channel and the presence of a click

 

indicates a Fock state with one or more photons. This limitation corresponds to the modern capabilities of measuring equipment. The algorithm we have developed allows us to consider the measurement possibilities in the optimal scheme search.

The paper is structured as follows. In Sec. II we analyze some well-known schemes in the KLM protocol. We describe the heralding procedure in terms of conditional probabilities, which reveals parameters for further optimization. We also discuss the change in heralding characteristics when the detector is a photon-number-resolving (PNR) one. Section III is dedicated to the genetic algorithms and their implementation for the task of an optical scheme search. We describe two series of experiments: optimizing the total actuation probability with no regard for the quality of heralding signal and optimizing the actuation probability with absolutely reliable heralding. Both series of experiments produce schemes, which we analyze in Secs. III D and III E. In Sec. IV we summarize and present our interpretation of the results.

All optical schemes discussed in this paper were analyzed and tested using the LOQC TECH web application [28].

## II. PROBABILITY ANALYSIS IN THE KLM PROTOCOL

### A. Qubit encoding and state space

Building a universal quantum computer means fulfilling the set of conditions called DiVincenzo criteria [29]. Photonic systems painlessly satisfy most of the criteria, leaving only one for consideration: the implementation of universal set of quantum gates [30]. For qubits, this universal set consists of three one-qubit rotations on the Bloch sphere and one two-qubit entangling gate. The choice of photons as a platform for computations makes single-qubit operations easy with waveplates and polarizing beam splitters. Two-qubit entanglement, in contrast, seems hard if even possible, since photons do not interact with each other under normal conditions. This interaction can in principle be achieved through nonlinear optical media [31], but it is too weak to be considered as a gate implementation resource. The most promising approach for the task of two-qubit gate implementation on photons is the KLM protocol [8], where photon interference occurs on linear optical elements and the gate actuation has essentially probabilistic nature.

In the KLM protocol each qubit is encoded as a photon location in two spatial modes: $|0\rangle$ corresponds to the photon being in one mode and $|1\rangle$ in the other. This encoding can be easily obtained from polarization encoding, where horizontal polarization of a photon encodes $|0\rangle$ and vertical $|1\rangle$.

The spatial modes which encode qubits (the signal modes) are supplemented by ancillary modes, possibly carrying ancillary photons. The particular pattern of photon detection on the output of ancillary modes represents the heralding signal of the gate actuation. The numbers of ancillary modes and ancillary photons depend on the gate implementation. They expand the state space of the system and the detection of ancillary photons on the output reduces it back to that represented by signal modes.

The photons in the signal modes can violate the qubit encoding by grouping in one mode or leaving to ancillary modes. Despite the fact that the presence of two photons in the signal mode at the output indicates that the gate is actuated incorrectly and takes the quantum state out of the two-qubit space, the phenomenon of photon bunching itself is an integral part of quantum interference and is always present in the schemes of entangling operations.

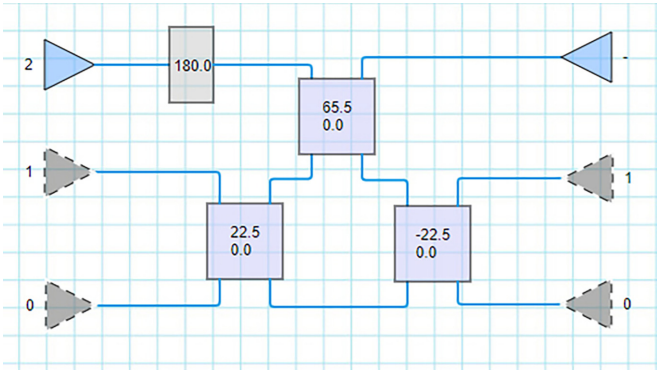


FIG. 1. The $NS_x$ gate. Our notation for the schemes is as follows: Blue triangles denote inputs and outputs of the signal modes and gray dashed triangles represent inputs and outputs of ancillary modes. Photons paths go from left to right. Numbers near the inputs denote the number of input photons in the corresponding mode. Numbers near the ancillary outputs specify the number of photons to be detected for the correct heralding signal (the heralding pattern). Gray rectangles represent phase shifters with angle $\phi$ specified inside the rectangle. Purple squares stand for beam splitters with $\theta$ in the first row and $\phi$ in the second.

The evolution of the quantum state is performed by linear optical elements: beam splitters and phase shifters. A phase shifter $P_\phi$ acts on one mode by changing its phase: $P_\phi|x\rangle = e^{i\phi}|x\rangle$. A beam splitter $B_{\theta,\phi}$ acts on two modes, performing the following unitary transformation:

$$B_{\theta,\phi} = \begin{pmatrix} \cos\theta & -e^{i\phi}\sin\theta \\ e^{-i\phi}\sin\theta & \cos\theta \end{pmatrix}. \tag{1}$$

The angle $\theta$ thereby affects the beam-splitter transparency, with $\cos\theta$ the reflection amplitude coefficient and $\sin\theta$ the transmission amplitude coefficient. The angle $\phi$ represents the relative phase shift between two outcomes.

The beam splitter acts on two different modes, so it is our main resource for entanglement. The CZ gate from [8] [we will refer to this gate as CZ(1/16) in future analysis and gate comparisons], for example, uses $B_{45^\circ,0}$ to collect photons from two different modes in one mode (the effect of photon bunching primarily discovered in [32]). In this case, as mentioned earlier, we go beyond the two-qubit logic, since in many schemes of entangling transformations, the dimension of the Hilbert space used is greater than the dimension of the two-qubit space. To eliminate this feature, we must be able to distinguish and discard those output states that are not the desired result of the gate action.

### B. Heralding event based on photon detection

Let us consider the heralding mechanism with the example of the $NS_x$ gate from [8] (Fig. 1). It has one signal mode (the first one, with the blue triangle denoting its input) and two ancillary modes (2 and 3, with gray dashed triangle inputs).

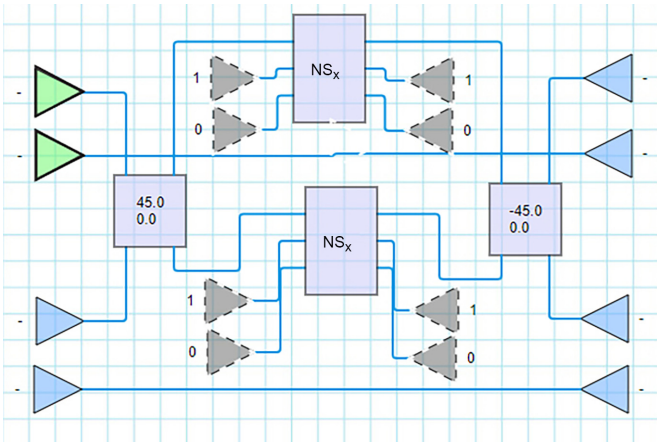


FIG. 2. Gate CZ(1/16), based on two $NS_x$ gates. Green bold inputs denote control qubit modes.

The state in the first mode is only transformed when it has two photons, in which case it changes its phase by $\pi$. The correct gate actuation coincides with the particular detection pattern on ancillary modes. This detection pattern indicates one photon in mode 2 and zero photons in mode 3. When this heralding signal is obtained one can be sure about the correct gate actuation, which for this particular scheme happens with a probability of $\frac{1}{4}$. The CZ(1/16) gate uses two $NS_x$ gates (Fig. 2).

The heralding pattern of CZ(1/16) is formed by heralding patterns of both $NS_x$, thus giving the probability of correct heralding 1/16. Here we arrive at an important point: In general, there is a difference between the probability of a correct heralding signal and the correct gate actuation. Let us introduce the following notation: $P$ denotes the probability of correct actuation, $P_a$ the probability of correct heralding signal, and $P_b$ the conditional probability of correct actuation when the correct heralding event happened. Then $P = P_a P_b$. If photon-number-resolving detectors are used for heralding in CZ(1/16), then for this scheme $P = P_a = 1/16$, with $P_b = 1$.

### C. Heralding event based on coincidence registration

Let us consider the CX gate scheme introduced in [10]. This gate has a better actuation probability of 1/9 (Fig. 3); hereafter we will refer to it as CX(1/9). However, this actuation probability does not fully rely on heralding, since the correct heralding signal (zero photons in the auxiliary modes) for this scheme is not accompanied by 100% correct actuation and $P_b < 1$ (see Fig. 4).

Thus, for the input states $|0_c, 0_t\rangle$ or $|0_c, 1_t\rangle$ (the subscript $c$ denotes control qubit and $t$ target) the conditional probability of correct actuation is when the correct heralding event happened, $P_b = 0.25$, and for inputs $|1_c, 0_t\rangle$ or $|1_c, 1_t\rangle$, $P_b = 0.5$. Here we denote the qubit logical states $|0_c\rangle$ and $|1_c\rangle$ by Fock states $|01\rangle$ and $|10\rangle$ in the first dual-rail mode, respectively. The target qubit states are denoted similarly with respect to the second dual-rail mode. Unlike in the case of CZ(1/16), the heralding pattern alone is unreliable for this gate.

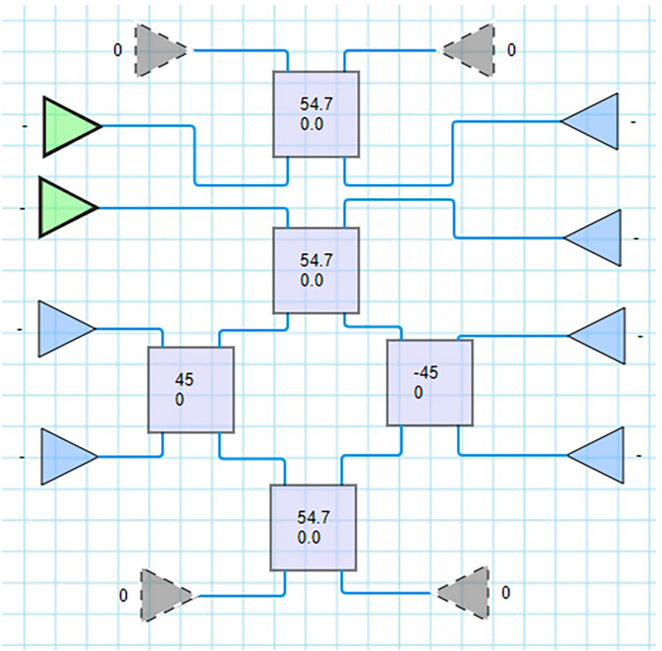


FIG. 3. Scheme of CX(1/9).

O'Brien *et al.* [10] proposed another heralding mechanism, that is, to distinguish the success of the operation by the presence of coincidences between the acts of detecting single photons in spatial modes encoding the states of qubits. This leads to a significant inconvenience when performing computational operations: One cannot be sure whether the gate has actuated correctly until the end of the entire calculation (which may consist of many gates). In addition, the measurement of coincidences tightens the requirements for signal synchronization. In gates which rely on photon counting, we have to ensure synchronization only for the elements with two-photon interference, but in circuits with a coincidence count, signal synchronization should be maintained until the final measurement.

Moreover, the schemes with coincidental heralding are difficult to scale. With a cascade of several gates, the presence of coincidences between photocounts in signal modes does not guarantee the correct operation of the entire cascade, since the correct heralding signal may be revealed when one of the gates does not work correctly also in the case of the correct operation of the entire circuit (we will discuss this problem in more detail in Sec. III F).

### D. Photon detection

Let us note that photon-number-resolving detectors are not always an undoubtedly implementable resource. It is more realistic to consider the possibility of distinguishing just two outcomes: One or more photons are detected or no photons are detected in one mode. In this case the probability $P$ of CZ(1/16) actuation does not change, but its components $P_a$ and $P_b$ shift and become dependent on the input state (Fig. 5). If we cannot discern one photon from two on the output of the ancillary modes, the heralding signal becomes less reliable.

From Fig. 5 one can conclude that for the input $|0_c, 0_t\rangle$ probabilities $P_a$ and $P_b$ do not change, but for other inputs they

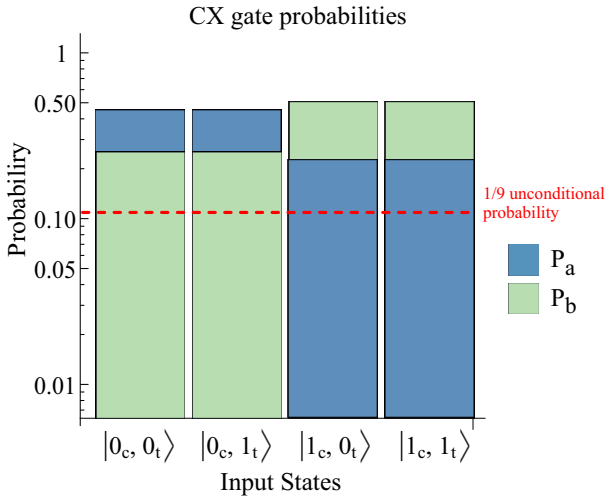


FIG. 4. Probabilities $P_a$ and $P_b$ for CX$(1/9)$. The heralding pattern is the absence of photons in ancillary outputs.

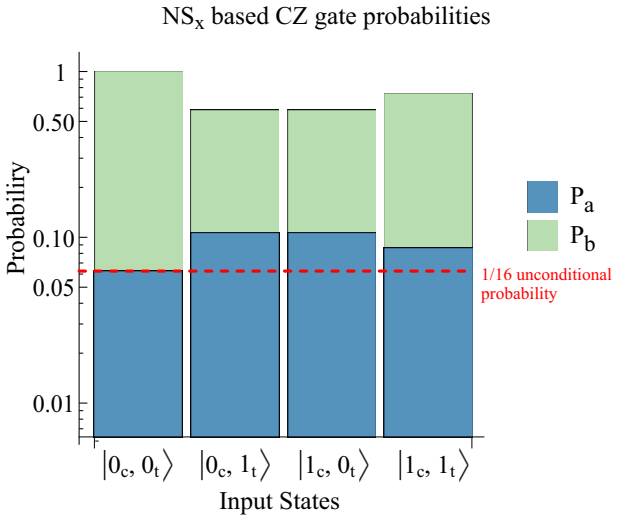


FIG. 5. Probabilities $P_a$ and $P_b$ of CZ$(1/16)$ for the case of non-photon-number-resolving detectors.

do, and an increased probability of a correct heralding event $P_a$ decreases the conditional probability $P_b$ of correct gate actuation. This depreciates the superiority of CZ$(1/16)$ over CX$(1/9)$ in terms of reliable heralding, possibly making the latter more appealing due to the better actuation probability.

Thus we find ourselves in need of a criterion for gate evaluation based on the gates' actuation probability components. The previous reasoning shows that the total probability of the gate triggering is not a sufficient parameter for optimizing the scheme. The conditional probability $P_b$ is an important parameter for scaling, but, as it was shown earlier, its relevance for the scheme input varies for the different schemes. The lowest and highest values of $P_b$ on the inputs of the computational basis can provide some insight into the scheme's heralding mechanism performance, but they become much less useful if the logical basis changes.

It is easy to show that the mean value of $P_a$ over any orthonormal basis is independent of the basis choice. Let us denote it by $\bar{P}_a$:

$$\bar{P}_a = \frac{P_a(|00\rangle) + P_a(|01\rangle) + P_a(|10\rangle) + P_a(|11\rangle)}{4}.$$

If the input of the scheme is considered a random event with uniform distribution, then $\bar{P}_a$ becomes the expected value of the correct heralding signal. Most quantum algorithms perform a Hadamard transformation at the start of the computation, thus preparing this uniform distribution of all possible inputs in the computational basis. In this case the probability of the heralding event $P_a$ equals $\bar{P}_a$.

For the conditional gates considered in this paper, the conditional probability $P_b$ is a function of $P_a$:

$$P_b = P/P_a.$$

Let us introduce $\bar{P}_b$, the expected value of correct gate actuation with a correct heralding signal for the case of a uniform distribution of inputs:

$$\bar{P}_b = P/\bar{P}_a = E(P_b).$$

Based on the above, we choose $\bar{P}_b$ to be our criterion for scheme evaluation. For example, for the gate CX$(1/9)$ it can be computed as follows:

$$\bar{P}_a = \frac{2/3 + 2/3 + 2/9 + 2/9}{4} = 4/9,$$

$$\bar{P}_b = \frac{1/9}{4/9} = 1/4.$$

We will use these characteristics to evaluate the proposed transformation schemes further.

## III. GENETIC ALGORITHMS FOR THE LINEAR OPTICS QUANTUM GATE SEARCH

### A. Principle of operation of genetic algorithms

The genetic (or evolutionary) algorithm introduced in [22,23] is the heuristic approach for the global optimization problem. It benefits from the idea of natural evolution, which seems very successful in the optimization of living species in nature. The simple idea of the algorithm is as follows.

*Step 1: Initialization.* Produce the set of random species, that is, the elements of the search space (the first generation).

*Step 2: Selection*. Evaluate each species in the generation (according to some fitness function) and choose a subset of the best of them.

*Step 3: Crossover*. Produce the offspring (the next generation) of the selected species by random recombination of their genetic material.

*Step 4: Mutations*. Apply random changes to the species of the new generation.

*Step 5.* Go to step 2 with the new generation.

### B. Tuning of numerical experiment parameters

In our experiments the species represent optical schemes for conditional quantum gates. Each such scheme has four signals and an arbitrary number of ancillary modes. Four signal modes represent two qubits: the control and the target

one. For each experiment, several parameters are chosen: The generation size $G$ is the number of species in one generation, the number of parents $G_p$ is the number of the best species in the generation that are chosen to produce offspring, the mutation rate $R$ corresponds to the probability of random changes of each species during the mutation step, the scheme depth (or complexity) $d$ accounts for the number of beam splitters in each scheme, $N_a$ is the number of ancillary modes, and $n_a$ is the number of photons in ancillary modes.

Each optical scheme is represented by an array of numbers (the species' genome). This genome consists of several parts, each responsible for particular information about a scheme: For $\theta$ rotation angles, there are $d$ numbers, one for each beam splitter in the represented circuit; for $\phi$ rotation angles, there are phase rotations in beam splitters and phase shifters; for mode numbers, there are $d$ pairs of numbers specifying the input modes for each beam splitter and up to $2d$ numbers for phase shifters; for ancillary inputs, there are $n_a$ mode numbers, one for each ancillary photon input; and for ancillary outputs, there are $n_a$ mode numbers, one for each ancillary photon detection. Rotation angles are specified in grades with precision up to two decimal points.

In the initialization step, we generate $G$ random genomes representing the optical circuits. The selection step requires a fitness function for species evaluation. We imply that this function optimizes two values: the fidelity of a conditional gate scheme and the probability of the gate actuation.

In the first set of experiments, described in Sec. III C, our goal is to find the best actuation probability $P$ among high-fidelity schemes. In that part of the research we set aside the heralding probability $P_a$ and conditional probability $P_b$. Then, in the second set of experiments (Sec. III E), we concentrate on the search for schemes with good heralding, those having $P_b = 1$. The goal is to find the best probability of schemes which allow scaling. In fact, such a search answers the question of what the maximum probability $P$ is of an actuation of a two-qubit gate that works with 100% probability if the correct heralding event occurs.

For the crossover step we also choose different approaches for different sets of experiments: single-point crossover, which selects a random point in the genome and generates the child by taking all genetic material before that point from parent 1 and the remainder from parent 2, and uniform crossover, where the parent is chosen randomly for each gene. Single-point crossover has proven to be the best choice for the first set of experiments, since the information about each optical element is stored locally in the scheme's genome. Splitting a genome at just one random point causes a high probability of passing successful parts of the scheme to the offspring as a whole. In the second set of experiments we modify the genome encoding to improve the speed of the scheme analysis. The description of each optical element becomes scattered across the whole scheme, thus making uniform crossover the most natural choice.

Our code for all experiments is available on GitHub [33]. In the first set of experiments we used the PYGAD library [34] for the genetic algorithms; then we had to develop our own implementation to enable CUDA. We also used the development language PYTHON 3.8.

The first set of experiments (on CPU) were run on an AMD Ryzen 5 3600 6-core processor with 32 Gb memory; GPU was not used. For the second set (with CUDA and GPU) we used Google Colab with a GPU-enabled runtime.

### C. Experimental set 1: Actuation probability optimization

For the first set of experiments we used generation size $G = 5000$, the number of mating parents $G_p = 800$, and the mutation rate introduced with assigning random values to the quarter of genes with probability 0.5. We started with scheme complexity $d = 8$ and the number of ancillary modes $N_a = 4$. Numbers $d$ and $N_a$ were chosen to allow the CZ(1/16) gate or a similar one to be found. Single-point crossover was used for the crossover step.

We needed the fitness function $f_1$, used on the selection step, to optimize two parameters: actuation probability $P$ and fidelity $F$. We used different approaches to combine these values, including multiplying them in different powers and exponentiation, but the best results were achieved with the threshold function, whereby one parameter is optimized up to a certain threshold and then the other parameter is optimized:

```
def f_1 (P, F):
    if P < P_min:
        return P
    return 1000 * F.
```

The function $f_1$ defined this way strongly favors fidelity over probability and excludes all low-probability schemes ($P < P_{\min}$) from consideration by giving them low fitness values. For the schemes with affordable probability $P \geqslant P_{\min}$ better fidelity wins regardless of probability. We set $P_{\min} = 0.1$ to be able to find gates like CX(1/9) or better.

The stopping criterion for the algorithm was reaching the fidelity value of 99%. After that we used LOQC.TECH [28] for the best scheme analysis and tuning. After a few experiments we excluded phase shifters from the genome representation and replaced them with beam splitters, since phase shifters did not affect the entanglement logic and occupied a significant part of the genome, consuming computing resources.

The first issue we noted was that the chosen set of parameters produced significant genetic garbage (that is, optical elements which do not affect the scheme performance). One of the examples can be found in Fig. 6. This looks very natural since evolution does not have instruments for eliminating something that does not affect survival.

The other notable point was that literally all schemes that survive selection have beam splitters on modes 1 and 3 with $\theta$ close to 50°–60°. Removing insignificant beam splitters and attuning the angles of the remaining ones gave us a scheme with a good fitness value just on three beam splitters.

Since an extensive search in the space of schemes with at most eight optical elements gave us the scheme with just three beam splitters, we decided to repeat the experiment with at most three beam splitters. Our reasoning is as follows: Three beam splitters is the minimal number of entangling elements for entangling two qubits in four spatial modes and more beam

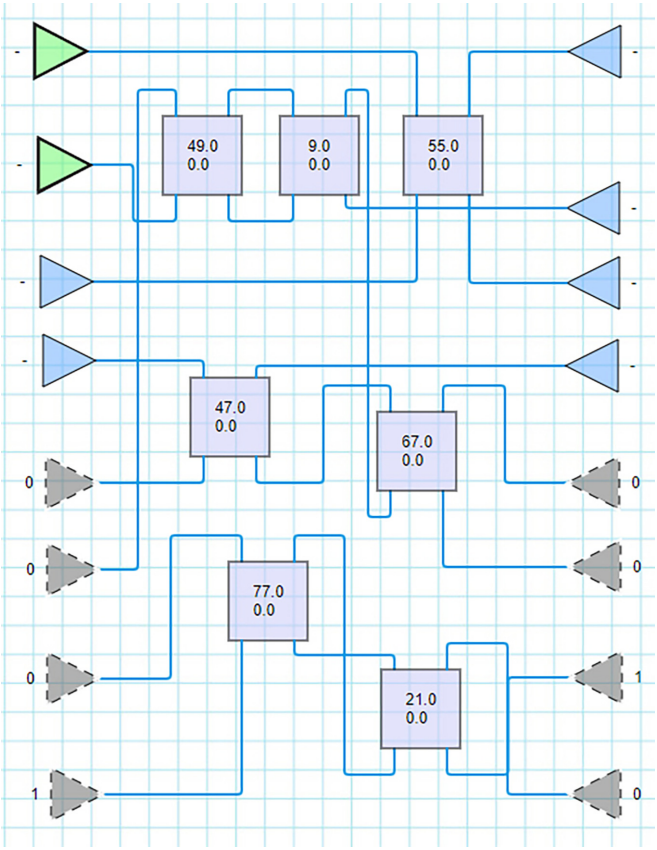


FIG. 6. Scheme of the CZ gate, with fidelity $F = 0.991\,87\ldots$ and probability $P = 0.0635\ldots$, obtained after 189 generations over 99 computation hours.

splitters produce more wrong paths for photons to follow, thus reducing the actuation probability of a gate.

We also increased the precision for $\theta$ by one decimal digit. After 11 days the algorithm stopped reaching the stopping criterion for fidelity equal to 0.999 and produced the scheme in Fig. 7. This scheme entangles the first modes of control and target qubits, while the second modes of both qubits are entangled with their own ancillary mode. With angles $\theta = \arccos\frac{1}{\sqrt{3}}$ the scheme reaches the best possible fidelity $F = 1$ with actuation probability $P = 1/9$ and implements the CZ transform.

We analyzed this found gate [hereafter referred to as CZ(1/9)] with the new metric introduced earlier in Sec. II E and obtained the same results as for CX(1/9), though the values of $P_a$ are slightly different for the basis inputs:

$$
\begin{aligned}
&P_a(|00\rangle) = 1/9,\\
&P_a(|01\rangle) = 1/3,\\
&P_a(|10\rangle) = 1/3,\\
&P_a(|11\rangle) = 1,\\
&\bar{P}_a = \frac{1 + 1/9 + 1/3 + 1/3}{4} = 4/9,\\
&\bar{P}_b = \frac{1/9}{4/9} = 1/4.
\end{aligned}
$$

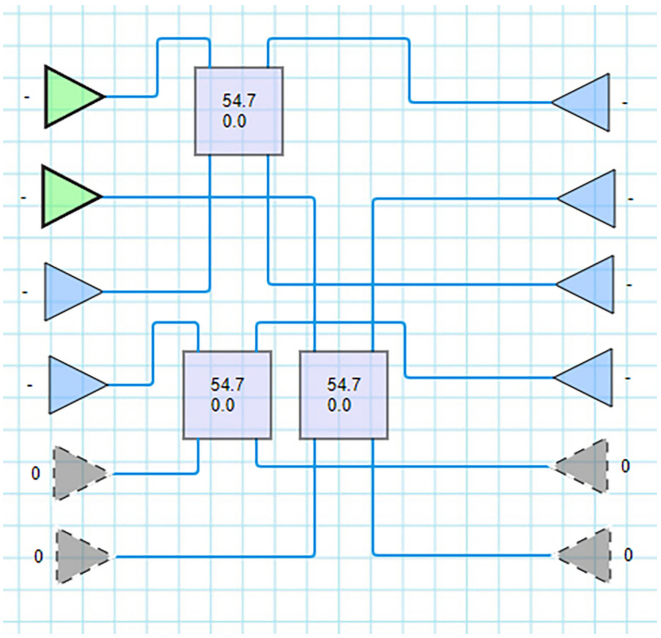


FIG. 7. Scheme of the CZ gate, with fidelity $F = 1$ and actuation probability $P = 1/9$.

This result gave us certainty about the applicability of the chosen search technique for our task.

### D. Experiments with gradient descent

For the second set of experiments we planned a search of schemes with good heralding, those having $P_b$ equal to 1 or close to it on all legitimate inputs, such as CZ(1/16). However, with the settings of the first experiments set, we found nothing close to this goal. The search space was too large and the iterations were too slow. We chose two different approaches to address this problem: optimizing the algorithm implementation and narrowing the search space. The second approach is the subject of this section.

To narrow the search space we needed to find out at least something about the search goal. The genetic algorithm is a heuristic which allows us to address the problem of global optimization and like the majority of heuristics it is poorly justified. There is a set of well-justified methods based on the idea of moving in the search space in the direction of the loss function gradient. These are gradient-descent and various pseudogradient methods. Unfortunately, they are well justified only for the task of local optimization and with restrictions on the loss function.

The loss function must at least be differentiable for all its variables. This restriction does not allow us to use gradient methods for the search of scheme design (the places of optical elements on the scheme), since this design is represented by integers, that is, mode numbers. The search, however, is possible when the design is fixed and only the real parameters of the optical elements have to be attuned. The fixed design therefore must allow representation of any possible unitary transform, which means it has to be universal. Finding a gate representation in the universal design by gradient descent could allow us to acquire some knowledge about

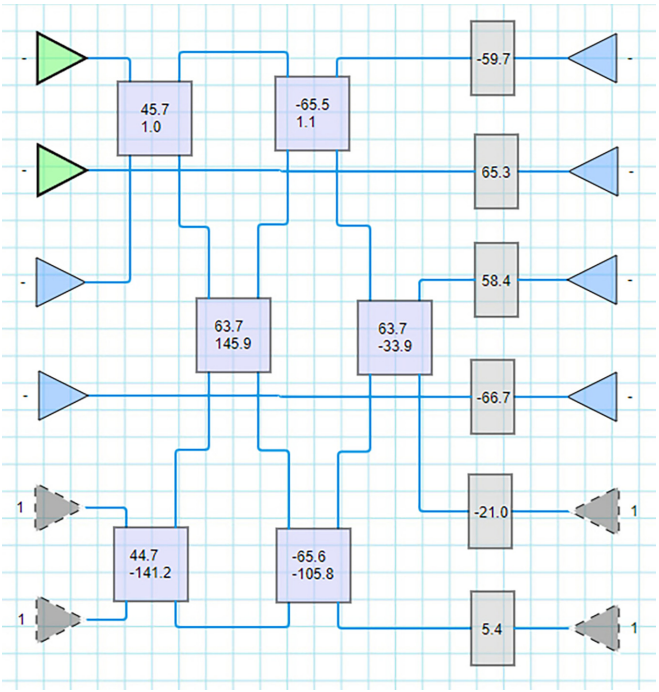


FIG. 8. Gradient descent result of the design of Clements *et al.*, with probability $P = 2/27$ and fidelity $F = 1$.

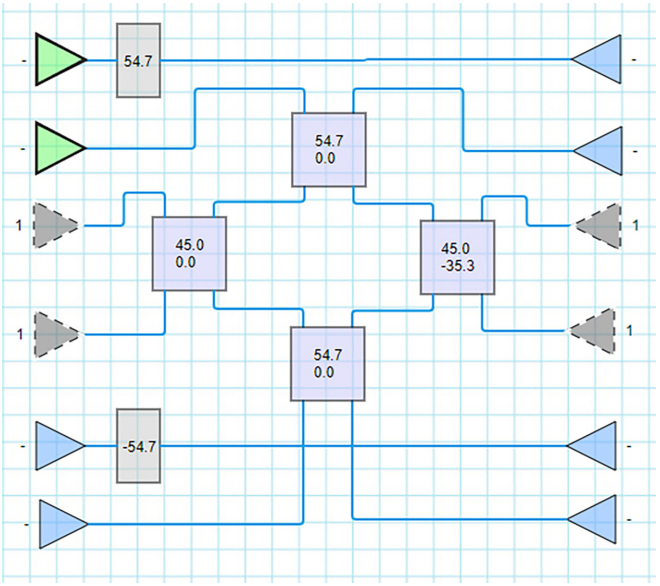


FIG. 9. Scheme of the CZ gate, with actuation probability $P = P_a = 2/27$, $P_b = 1$, and fidelity $F = 1$.

the parameters of the scheme for further search with genetic algorithms.

In this set of experiments we used universal designs introduced by Reck *et al.* [35] and Clements *et al.* [36] and our own, which is close to the design of Reck *et al.* but with a more convenient expression for the loss function. The initial scheme size was based on the scheme of CZ(1/16): four signal and four ancillary modes with two ancillary photons.

Local optimization methods make the choice of the initial point of iterations very important. Our strategy was to choose this point randomly for each launch; thus the vast majority of experiments ended up in local minima without reaching tolerable values of fidelity. It took some time before we found a scheme with fidelity close to 1 and an actuation probability of 2/27. This scheme was found in our own design, but with analysis of its structure we succeeded in finding it also in well-known designs from [35,36]. The scheme of the design of Clements *et al.* [36] is presented in Fig. 8.

This part of the research allowed us to adjust the settings of genetic algorithms and narrow the search space, thus making a significant step towards achieving a positive result with their application.

### E. Experimental set 2: Search of schemes with a good heralding signal

The first set of experiments gave us some interesting results, but they were not new and they took too much computing time to find. We decided to rewrite the code for the scheme evaluation and search with PYTORCH to employ the capabilities of modern GPUs. After we had done that, the CZ gate from the previous set of experiments took 11 s to find using Google Colab with a GPU-enabled runtime. We assumed that 11 s for what previously took 11 days is a rather satisfying speedup, so we were prepared to continue this research.

For the second set of experiments we carried out the following modifications of the previous settings.

(i) All schemes with $P_b < 1$ were discarded. We were concerned about a gate with a 100% heralding, which is very important in computation.

(ii) We allowed phase shifters in scheme genomes, since they are necessary for universality.

(iii) We chose scheme parameters to match those dictated by the results of gradient descent search: the scheme depth $d = 6$, the number of ancillary modes $N_a = 2$, and the number of ancillary photons $n_a = 2$.

We also redefined the fitness function in order to maximize probability and discard the low-fidelity schemes:

```
def f_2(P, F):
    if F < F_min:
        return F
    return 1000 * P.
```

The threshold for fidelity this time was rather high, $F_{\min} = 0.9999$, and we made sure that ancillary photons were detected in the same modes they were introduced into schemes. This significantly reduced the dimensions of the search space, while presumably eliminating its parts with low-fidelity species.

After 3 h of search on the GPU-enabled runtime the scheme was found with fidelity $F = 0.999\,996\ldots$ and probability $P = 0.738\ldots$. Removing genetic garbage and attuning the angles gave us the gate (Fig. 9) with actuation probability 2/27 and fidelity 1, which uses only four beam splitters and two phase shifters [hereafter referred to as CZ(2/27)], the same actuation probability and number of optical elements the gate from [9] has, though the designs of these schemes are different.

TABLE I. Comparative analysis of the schemes discussed in this paper.

| Comparison parameters | CZ(1/16) (Fig. 2) | CZ(1/9) (Fig. 7) | CZ(2/27) (Fig. 9) |
|---|---|---|---|
| scheme depth $d$ | 8 | 3 | 4 |
| $P$ | 1/16 | 1/9 | 2/27 |
| $\bar{P}_b$ | 1 | 0.25 | 1 |
| $\bar{P}_b$ with non-PNR detectors | 0.689... | 0.25 | 0.639... |
| $\bar{P}_b$ after the correction procedure | 1 | 0.25 | 1 |

We provide a comparative analysis of the schemes discussed in this paper in Table I. The CZ(1/9) gate is the best in regard to actuation probability and simplicity (the number of optical elements). It has however a comparatively poor heralding mechanism. As was shown in Sec. II C, it is not completely appropriate for computations which usually demand repetitive applications of conditional gates. The champion among the schemes with a good heralding signal is the CZ(2/27) gate, in both the actuation probability and the scheme simplicity.

### F. Heralding mechanism correction for non-PNR detectors

We have shown in Sec. II D that the conditional probability of gate actuation $P_b$ can decrease when non-photon-number-resolving detectors are used. In this section we show how one can address this problem for the gates like CZ(2/27), assuming we can distinguish only two outcomes of detection in auxiliary modes: no photons or one or more photons.

Below we will show how to correct the situation and restore the conditional probability $P_b$ using an additional measurement in the proposed CZ(2/27) scheme. With analysis of all possible outcomes in the presence of photons in ancillary modes, one can conclude that incorrect gate actuations are associated with the leakage of photons from the qubit modes to the auxiliary ones. Such leakage is inevitably accompanied by the loss of the qubit state in the signal modes. We propose to supplement the scheme with one additional heralding measurement. After detecting the required pattern on the ancillae, one should check for coincidences at the two outputs of the control qubit modes $C-C$ (outputs 1 and 2 counting from the top in Fig. 9). After that one should perform a similar measurement with the two outputs of the target qubit modes $T-T$ (outputs 5 and 6 in Fig. 9). According to the measurement results, we discard the results for which there are coincidences (that is, there is a lack of photons at both control and target outputs). Such a measurement restores the value of the conditional probability of the correct scheme actuation $P_b = 1$.

It should be noted that such a check is possible due to the peculiarity of our scheme. With a correct heralding signal on ancillae, one can never detect photons in the signal mode if no photons were introduced into this signal mode. The photon from the control mode cannot get into the target one and vice versa. This fact indicates another remarkable feature of this check: It does not interfere with the scalability of calculations, that is, it can be carried out once at the end of calculations, after a chain of several gates.

Let us consider the described procedure in more detail. For example, let the state $|0101\rangle$ be initiated on the input of the CZ(2/27) gate. At the output of the scheme, we check the pattern on the ancillae. Among the possible erroneous outcomes that we could not distinguish, there is an outcome when two photons are present in one of the ancillae and another photon is present in the other. At the same time, in one of the signal modes of the output state (for example, in the target) there will be zero photons in both channels. Without performing any additional actions, we send the result to the input of the second similar scheme CZ(2/27). The state $|0100\rangle$ evolves in the second scheme, after which we check the pattern again on the ancillae of the second scheme. The chain of gates can be of the required length. For the selected variants, we check not only the heralding pattern on the ancillae, but also the matches in the $C-C$ and $T-T$ channels, at the output of the chain. All options will be eliminated based on the presence of a no photon–no photon match, that is, the presence of an incorrect operation in one of the gates could always be distinguished at the output.

It is important to note that although the proposed check looks similar to the one implemented in the CX(1/9) and CZ(1/9) schemes, these schemes do not allow us to filter out incorrect actuations at one gate from the chain by the final measurement. For example, taking the state $|1010\rangle$ at the input of the CZ(1/9) gate as one of the possible options, we will get the state $|2000\rangle$ at the output. According to the ancilla pattern for this scheme, we do not recognize an incorrect actuation. If such a state enters the second similar gate from the chain, it can turn into $|1010\rangle$ at the output, and by monitoring coincidences we will not recognize that one of the gates in the chain worked incorrectly. Such a defect is associated with the possibility of photon migration from the control mode to the target mode and vice versa during the evolution of the state. Note that the CZ(1/16) protocol and CZ(2/27) gates do not allow photon migration between the target and control modes, which means that even if there are non-photon-number-resolving detectors, the heralding mechanism in this scheme can also be adjusted by an additional measurement of coincidences in the signal modes at the end of the calculation without compromising scalability.

## IV. CONCLUSION

In this research we presented the results of genetic algorithm application to the problem of a heralded, conditional, quantum gate, linear optic scheme search. With this approach we managed to find two high-fidelity optical schemes. One of these schemes has the best currently known actuation probability $P = 1/9$ with no regard for the heralding signal quality and the other has the best actuation probability $P = 2/27$ among the schemes with a good ($P_b = 1$) heralding mechanism.

The result of the first set of experiments convinced us that 1/9 is the best actuation probability for the conditional gates in the KLM protocol, assuming we do not have entangled ancillary photons. Increasing the number of ancillary modes as well as the number of photons in the ancillary modes only worsens the situation. The CZ(1/9) gate found with an

extensive search has the same characteristics as the CX gate analytically deduced in [10].

We also note that the gate actuation probability is not the only useful characteristic of an optical scheme. The quality of the correct actuation heralding event becomes much more important when one needs to perform computations placing several conditional gates in line with no intermediary measurements (except those in ancillary modes). We introduced the simple metrics which allowed us to compare the schemes with less than 100% heralding reliability, regardless of the logical basis, and applied this metrics for comparison with the optical schemes discussed.

In the second set of experiments we placed the restriction on the schemes to have a good heralding mechanism. As a result we found the CZ(2/27) gate, which has $P_b = 1$, fidelity $F = 1$, and actuation probability $P = 2/27$, the same characteristics as in [9], though with a different (and slightly simpler) design.

The results obtained show the prospects of the method of scheme analysis developed: Both circuits with record characteristics for certain parameters were found as a result of the genetic search.

All of the gate schemes considered require PNR detectors to obtain the correct heralding pattern, which is a questionably available resource at the present time. We analyzed the behavior of the considered optical schemes under the assumption that we cannot distinguish the actual number of detected photons. The heralding signal quality decreases in this case; thus we introduced the procedure to restore it for the CZ(2/27) gate and that found by Knill [9]. This procedure allows scaling of computations and requires the signal photon detection only at the end of computations where such detection is natural.

The fact that the schemes with the best-known characteristics were found with no additional insight shows that genetic algorithms are a prospective and useful instrument for linear optical scheme design for quantum computing. We believe that it will be successfully used further for this type of task and produce new fruitful results.

## ACKNOWLEDGMENT

This work was financially supported by the Russian Science Foundation (Grant No. 22-22-00022).

[1] S. Slussarenko and G. J. Pryde, Photonic quantum information processing: A concise review, Appl. Phys. Rev. **6**, 041303 (2019).

[2] Y. Wang, J. Li, S. Zhang, K. Su, Y. Zhou, K. Liao, S. Du, H. Yan, and S.-L. Zhu, Efficient quantum memory for single-photon polarization qubits, Nat. Photon. **13**, 346 (2019).

[3] Y. F Hsiao, P.-J. Tsai, H.-S. Chen, S.-X. Lin, C.-C. Hung, C.-H. Lee, Y.-H. Chen, Y.-F. Chen, I. A. Yu, and Y.-C. Chen, Highly Efficient Coherent Optical Memory Based on Electromagnetically Induced Transparency, Phys. Rev. Lett. **120**, 183602 (2018).

[4] P. Kok, W. J. Munro, K. Nemoto, T. C. Ralph, J. P. Dowling, and G. J. Milburn, Linear optical quantum computing with photonic qubits, Rev. Mod. Phys. **79**, 135 (2007).

[5] F. V. Gubarev, I. V. Dyakonov, M. Y. Saygin, G. I. Struchalin, S. S. Straupe, and S. P. Kulik, Improved heralded schemes to generate entangled states from single photons, Phys. Rev. A **102**, 012604 (2020).

[6] S. A. Fldzhyan, M. Y. Saygin, and S. P. Kulik, Compact linear optical scheme for Bell state generation, Phys. Rev. Res. **3**, 043031 (2021).

[7] H. F. Hofmann and S. Takeuchi, Quantum phase gate for photonic qubits using only beam splitters and postselection, Phys. Rev. A **66**, 024308 (2002).

[8] E. Knill, R. Laflamme, and G. J. Milburn, A scheme for efficient quantum computation with linear optics, Nature (London) **409**, 46 (2001).

[9] E. Knill, Quantum gates using linear optics and postselection, Phys. Rev. A **66**, 052306 (2002).

[10] J. L. O'Brien, G. J. Pryde, A. G. White, T. C. Ralph, and D. Branning, Demonstration of an all-optical quantum controlled-NOT gate, Nature (London) **426**, 264 (2003).

[11] R. Okamoto, H. F. Hofmann, S. Takeuchi, and K. Sasaki, Demonstration of an Optical Quantum Controlled-NOT Gate without Path Interference, Phys. Rev. Lett. **95**, 210506 (2005).

[12] N. K. Langford, T. J. Weinhold, R. Prevedel, K. J. Resch, A. Gilchrist, J. L. O'Brien, G. J. Pryde, and A. G. White, Demonstration of a Simple Entangling Optical Gate and Its Use in Bell-State Analysis, Phys. Rev. Lett. **95**, 210504 (2005).

[13] O. Gazzano, M. P. Almeida, A. K. Nowak, S. L. Portalupi, A. Lemaître, I. Sagnes, A. G. White, and P. Senellart, Entangling Quantum-Logic Gate Operated with an Ultrabright Semiconductor Single-Photon Source, Phys. Rev. Lett. **110**, 250501 (2013).

[14] T. C. Ralph, A. G. White, W. J. Munro, and G. J. Milburn, Simple scheme for efficient linear optics quantum gates, Phys. Rev. A **65**, 012314 (2001).

[15] T. C. Ralph, Scaling of multiple postselected quantum gates in optics, Phys. Rev. A **70**, 012312 (2004).

[16] J. Zeuner, A. N. Sharma, M. Tillmann, R. Heilmann, M. Gräfe, A. Moqanaki, A. Szameit, and P. Walther, Integrated-optics heralded controlled-NOT gate for polarization-encoded qubits, npj Quantum Inf. **4**, 13 (2018).

[17] T. B. Pittman, M. J. Fitch, B. C. Jacobs, and J. D. Franson, Experimental controlled-NOT logic gate for single photons in the coincidence basis, Phys. Rev. A **68**, 032316 (2003).

[18] S. Gasparoni, J.-W. Pan, P. Walther, T. Rudolph, and A. Zeilinger, Realization of a Photonic Controlled-NOT Gate Sufficient for Quantum Computation, Phys. Rev. Lett. **93**, 020504 (2004).

[19] Z. Zhao, A.-N. Zhang, Y.-A. Chen, H. Zhang, J.-F. Du, T. Yang, and J.-W. Pan, Experimental Demonstration of a Nondestructive Controlled-NOT Quantum Gate for Two Independent Photon Qubits, Phys. Rev. Lett. **94**, 030501 (2005).

[20] J.-P. Li, X. Gu, J. Qin, D. Wu, X. You, H. Wang, C. Schneider, S. Höfling, Y.-H. Huo, C.-Y. Lu, N.-L. Liu, L. Li, and J.-W. Pan, Heralded Nondestructive Quantum Entangling Gate with Single-Photon Sources, Phys. Rev. Lett. **126**, 140501 (2021).

[21] W. Gao, A. M. Goebel, C.-Y. Lu, H.-N. Dai, C. Wagenknecht, Q. Zhang, B. Zhao, C.-Z. Peng, Z.-B. Chen, Y.-A. Chen, and

J.-W. Pan, Teleportation-based realization of an optical quantum two-qubit entangling gate, Proc. Natl. Acad. Sci. USA **107**, 20869 (2010).

[22] N. A. Barricelli, Symbiogenetic evolution processes realized by artificial methods, Methodos **9**, 143 (1957).

[23] A. Fraser, Simulation of genetic systems by automatic digital computers. I. Introduction, Aust. J. Biol. Sci. **10**, 484 (1957)

[24] F. Curtis, X. Li, T. Rose, Á. Vázquez-Mayagoitia, S. Bhattacharya, L. M. Ghiringhelli, and N. Marom, GAtor: A first-principles genetic algorithm for molecular crystal structure prediction, J. Chem. Theory Comput. **14**, 2246 (2018).

[25] X.-N. Bui, H. Nguyen, Y. Choi, T. Nguyen-Thoi, J. Zhou, and J. Dou, Prediction of slope failure in open-pit mines using a novel hybrid artificial intelligence model based on decision tree and evolution algorithm, Sci. Rep. **10**, 9939 (2020).

[26] X.-N. Bui, H. Moayedi, and A. S. A. Rashid, Developing a predictive method based on optimized M5Rules-GA predicting heating load of an energy-efficient building system, Eng. Comput. **36**, 931 (2020).

[27] H. Liang, J. Zou, M. J. Khan, and K. Zuo, An improved genetic algorithm optimization fuzzy controller applied to the wellhead back pressure control system, Mech. Syst. Signal Process. **142**, 106708 (2020).

[28] LOQC.TECH: Linear Optics Quantum Computing project, https://loqc.tech

[29] D. P. DiVincenzo, The physical implementation of quantum computation, Fortschr. Phys. **48**, 771 (2000).

[30] A. Barenco, C. H. Bennett, R. Cleve, D. P. DiVincenzo, N. Margolus, P. Shor, T. Sleator, J. A. Smolin, and H. Weinfurter, Elementary gates for quantum computation, Phys. Rev. A **52**, 3457 (1995).

[31] X.-W. Wang, D.-Y. Zhang, S.-Q. Tang, L.-J. Xie, Z.-Y. Wang, and L.-M. Kuang, Photonic two-qubit parity gate with tiny cross-Kerr nonlinearity, Phys. Rev. A **85**, 052326 (2012).

[32] C. K. Hong, Z. Y. Ou, and L. Mandel, Measurement of Subpicosecond Time Intervals between Two Photons by Interference, Phys. Rev. Lett. **59**, 2044 (1987).

[33] https://github.com/sysoevss/galopy

[34] A. F. Gad, PyGAD: An intuitive genetic algorithm Python library, arXiv:2106.06158.

[35] M. Reck, A. Zeilinger, H. J. Bernstein, and P. Bertani, Experimental Realization of Any Discrete Unitary Operator, Phys. Rev. Lett. **73**, 58 (1994).

[36] W. R. Clements, P. C. Humphreys, B. J. Metcalf, W. S. Kolthammer, and I. A. Walmsley, Optimal design for universal multiport interferometers, Optica **3**, 1460 (2016).